Evidence for symmetry-reduction in solid H_2O above 222 GPa SUPPLEMENTARY INFORMATION

Ashkan Salamat[1,2], Zachary M. Grande[1,2], Victor N. Robinson[3], Dean Smith[4], Jesse S. Smith[4], Oliver Tschauner[5], and Burkhard Militzer[4]

[1]**Nevada Extreme Conditions Laboratory, University of Nevada, Las Vegas, Las Vegas, 89154, NV, USA**
[2]**Department of Physics & Astronomy, University of Nevada, Las Vegas, Las Vegas, 89154, NV, USA**
[3]**Department of Earth and Planetary Science, University of California, Berkeley, Berkeley, 94720, CA, USA**
[4]**HPCAT, X-ray Science Division, Argonne National Laboratory,Argonne, 60439, IL, USA**
[5]**Department of Geoscience, University of Nevada, Las Vegas, Las Vegas, 89154, NV, USA**

ABSTRACT

Observation of Post-ice X Phase in H_2O above 220 GPa

Keywords: Ice, High Pressure, Phase Transition, XRD

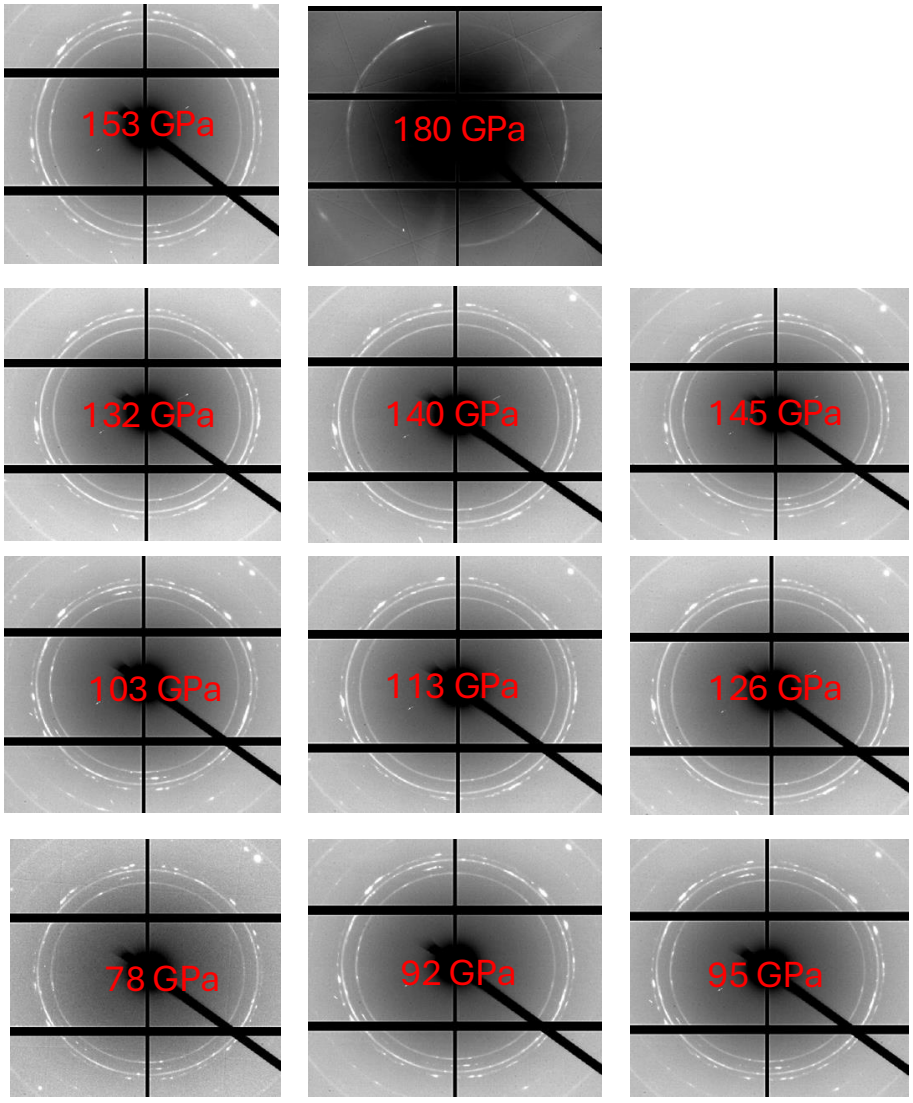

Figure 1. 2D XRD images of all the pressures up to 180 GPa, showing ice-X. The image at 180 GPa is from a different loading using 50 μm culets, whilst the rest shown used 30 μm culets.

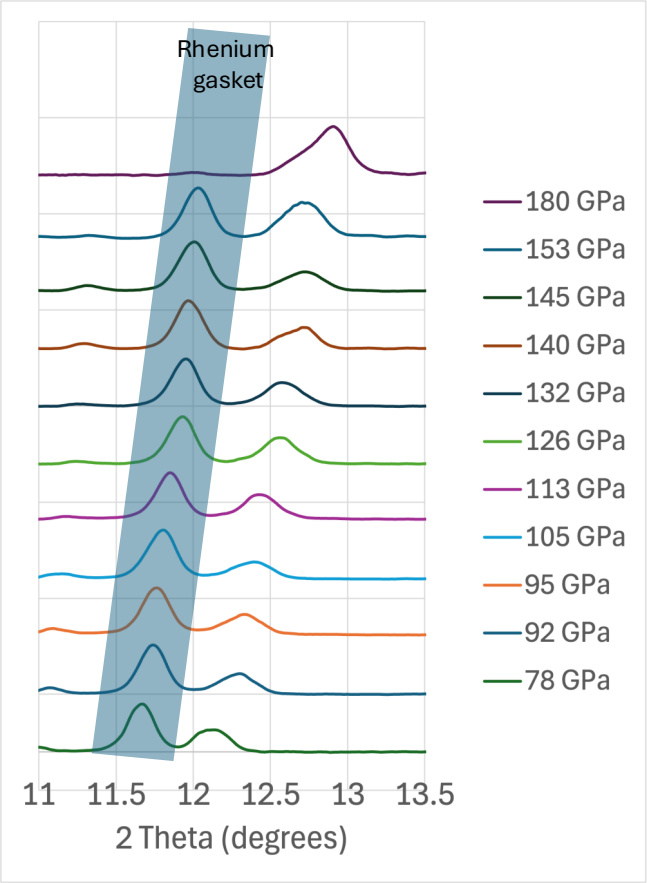

Figure 2. A stack plot of the integrated 1D projections of the 2D XRD images shown in Fig S1. The diffraction peak of interests is of ice-X, starting above 12 degree 2 theta. The presence of rhenium is highlighted through out the stack plot.

The X-ray beam at HPCAT 16-ID-B is focused using a 200 x 100 mm KB mirror assembly, producing a ∼1 x 1 μm beam with a predominantly Lorentzian intensity profile. This configuration is designed to deliver an on-sample flux of ∼1x10^{12} ph/s at 29 keV. Our experiments mostly utilize 30 μm culets with a ∼10 μm sample hole. The starting thickness of the gasket is 6 μm, thinning out to ¡1 μm by 200 GPa. Unlike most XRD studies, data collection is performed without rocking or raster scanning. Each XRD measurement is capturing a stationary image, as rocking the DAC would introduce a dominant rhenium gasket signal. Also, having such a small beam is suboptimal for powder averaging statistics. Consequently, our powder averaging is less uniform than in experiments where larger beam size and techniques like rocking on the center of rotation are used, and this must be considered when evaluating the powder statistics presented. For a Lorentzian beam profile with a 1 μm FWHM, the relative intensity at 5 μm from the center is ∼0.99% of the peak intensity. Given that rhenium's scattering power (5625) far exceeds that of oxygen (64), and with a ∼10 μm gasket width, the rhenium contribution to the diffraction signal is approximately 1:1 relative to the sample.

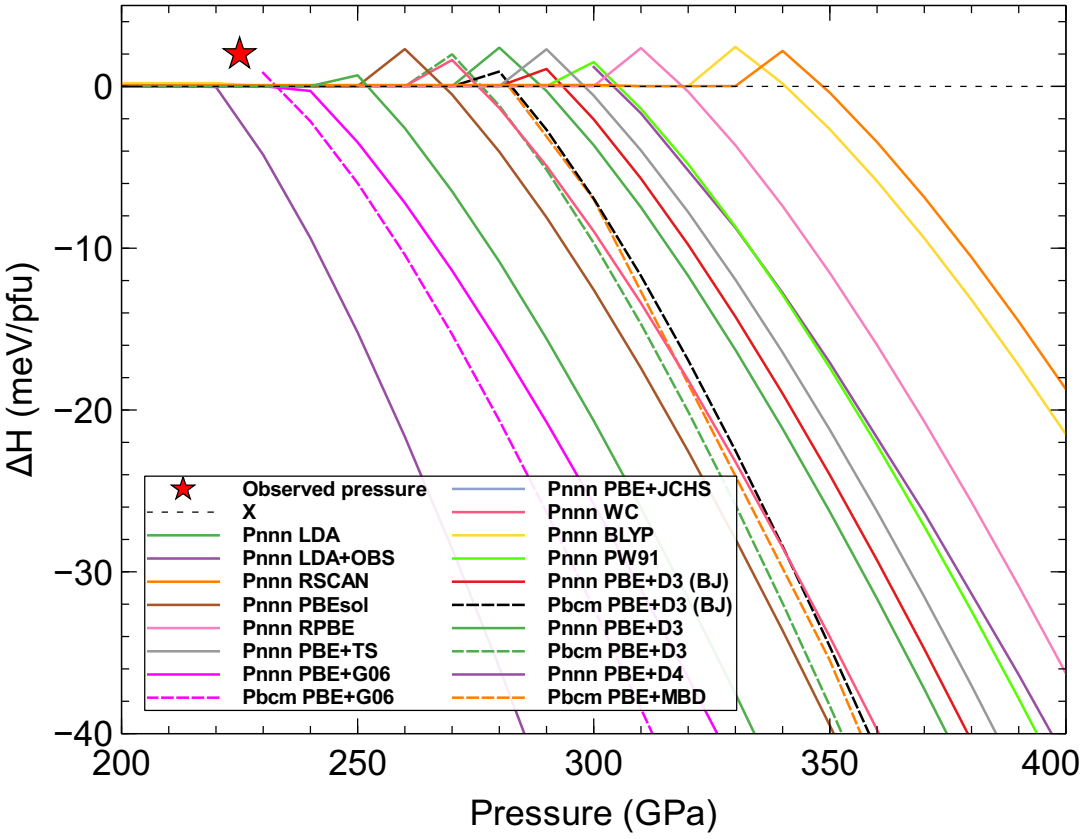

Figure 3. Relative enthalpy of $P4_2/nmm$ (*Pnnn*) and *Pbcm* phases to ice-X as a function of pressure for different DFT exchange-correlation functionals and dispersion corrections. The red star represents the transition pressure observed in this work.

1 DISCUSSION OF THE $P2_12_12$ STRUCTURAL SOLUTION

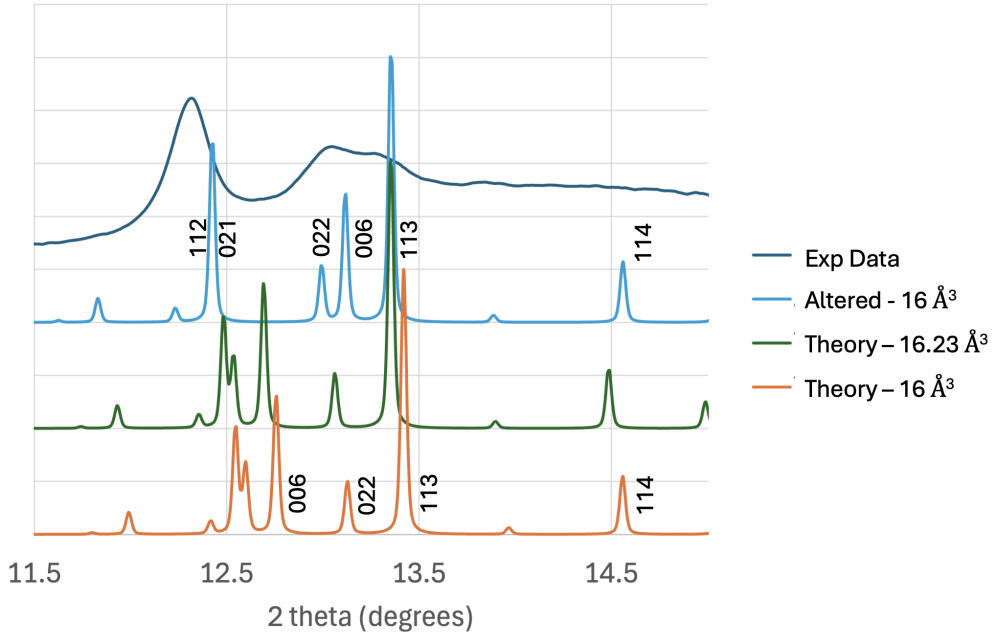

Figure 4. Simulated XRD patterns of varying $P2_12_12$ structures compared to the experimental data at 230 GPa. The two theory patterns are isotropically adjusted cell parameters by fixing volume at 16 Å^3 or matching the experimental XRD at 16.23 Å^3. Simulated XRD pattern (altered) shows the necessary cell parameter change to achieve the correct volume.

The $P2_12_12$ structure is energetically comparable to the other proposed solutions, making it a viable candidate for the observed symmetry lowering. Notably, it features an elongated c-axis, leading to additional predicted Bragg diffraction features compared to the competing *Pbcm* and $P4_2/nnm$ structures. This Bragg peak is not seen in the measured XRD pattern. The cell parameters are a = 2.325 Å, b = 3.759 Å, c = 10.980 Å, at 16Å^3/2 f.u. However, as shown in Figure 2a and the figure below, the $P2_12_12$ structure at the ice-X pressure value of approximately 230 GPa does not match the experimental data. To reconcile the theoretical structure with the experimental results, the unit cell must be expanded by at least 1.5%. This required volume expansion, along with the absence of relatively strong diffraction features between 12.5 and 12.75 in the figure below (around 3.4 Å^3 in Figure 2a), strongly suggests that the $P2_12_12$ structure in its theoretically cell geometry is not the correct interpretation of the observed symmetry lowering. The hkl values are assigned to the peaks of interest in the various adaptations of the $P2_12_12$ theoretical model. For an ideal unit cell with a volume of 16 Å^3, the peak at 12.8 degrees corresponds to the (006) reflection, while the peak at 14.6 degrees corresponds to (114). (hk0) texturing could eliminate the (006) peak, but this would also affect all other diffraction peaks. The (114) peak at 14.6 degrees is inherently linked to the dominant (113) peak. If the volume is fixed at 16 Å^3/2 f.u. and the unit cell adjusted to match the experimental data, the cell parameters must be distorted to a = 2.360 Å, b = 3.809 Å, c = 10.680 Å, compressing the c-axis while expanding the a- and

b-axes (Figure below). This distortion introduces a third distinct peak at 13 degrees that is not observed in our data. This is another reason for why we do not favor the $P2_12_12$ structure. The assigned hkl values to the altered XRD pattern to illustrate how the diffraction pattern changes in response to the distorted unit cell required to achieve the correct volume.

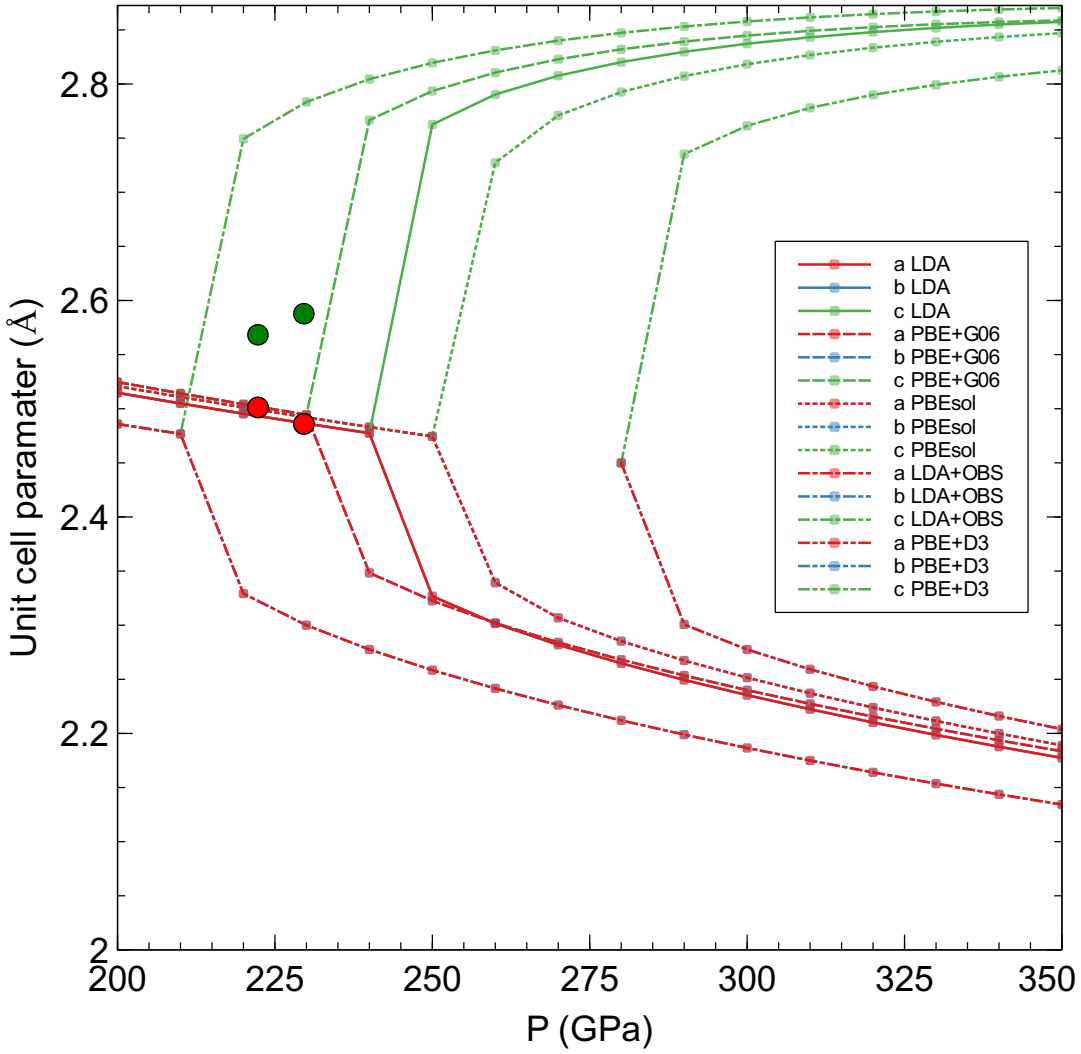

Figure 5. Unit cell parameters of $P4_2/nmm$ for different XC functionals. Large circles are from XRD.

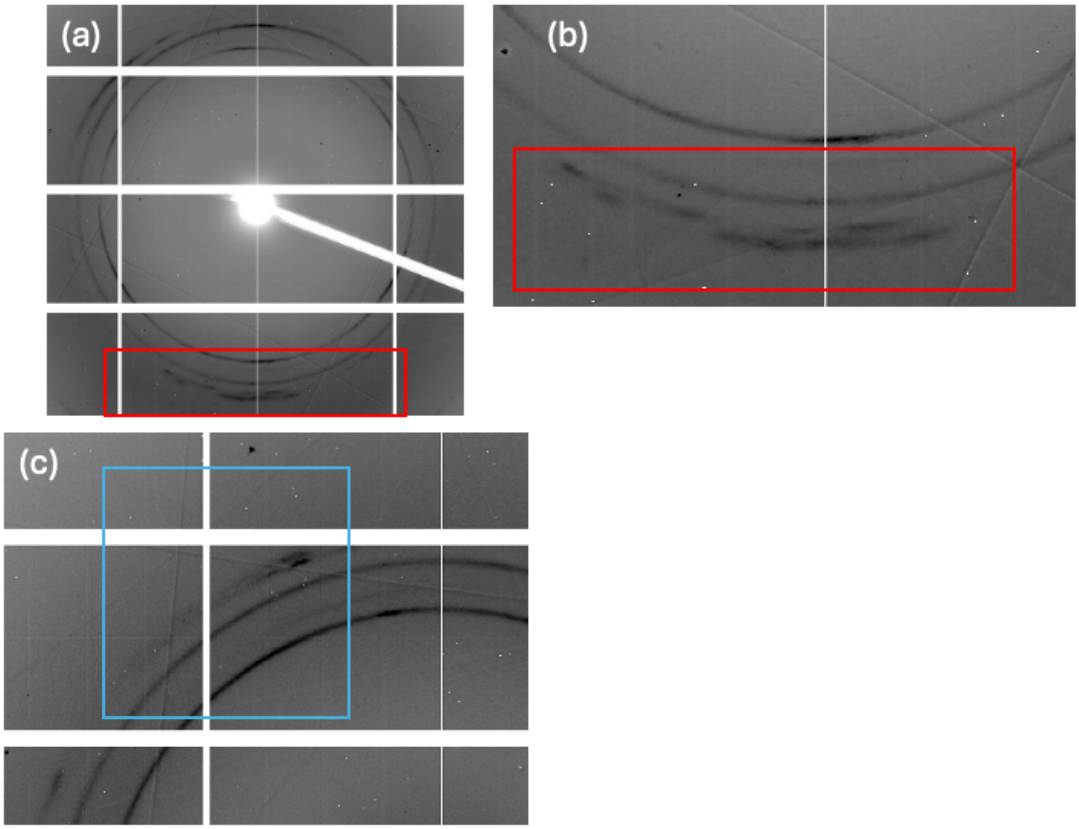

Figure 6. 2D XRD image taken at APS, HPCAT 16-ID-B at 230 GPa. (a) Full 2D image and (b) A close up of the region of interest from. The new features are highlighted in the red box. (c) A different measurement taken a few microns away from the center, sampling different orientations of the new phase (highlighted in blue box).

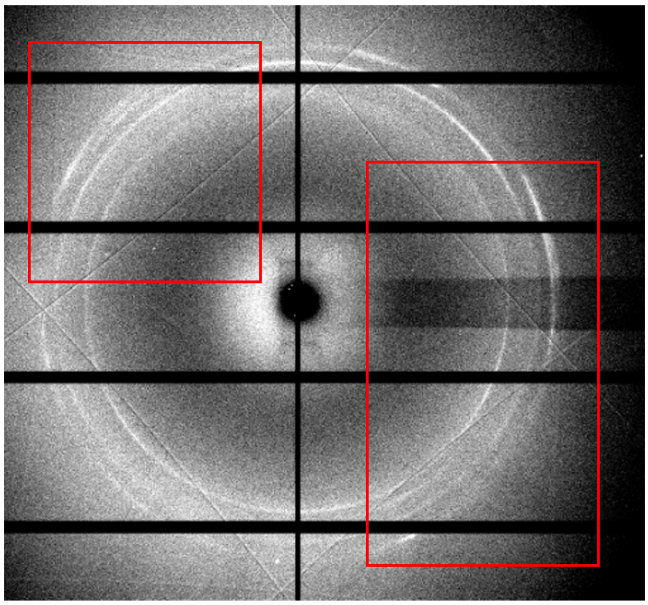

Figure 7. 2D XRD image taken at ALS beamline 12.2.2 16-ID-B at 230 GPa (highlighted in red box).

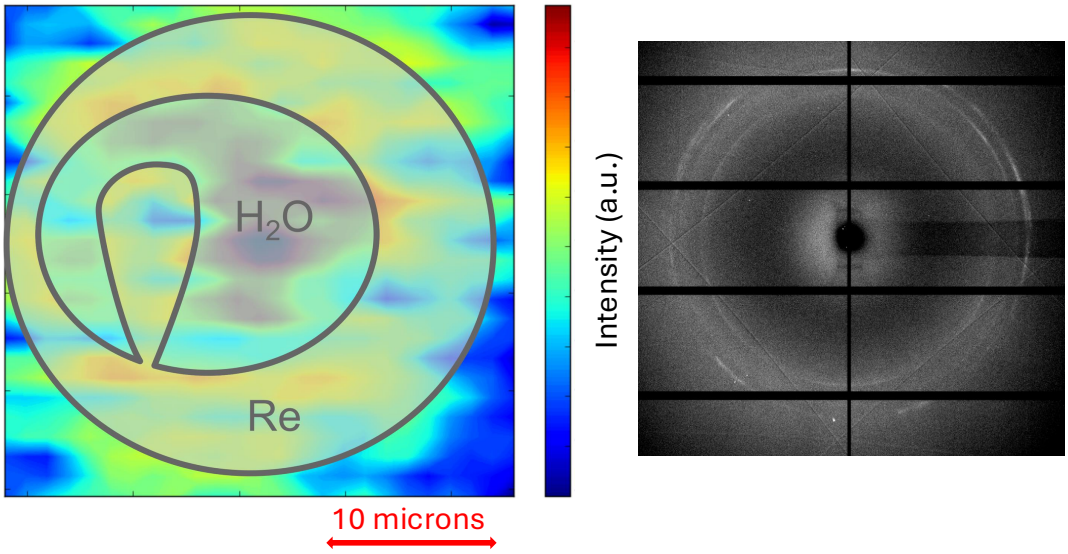

Figure 8. Understanding the gasket dimensions at 230 GPa. (left) 2D transmission imaging of the loading, carried out at beamline HPCAT-16-ID-B. It shows the gasket hole, sample, and the flake of rhenium that had protruded out into the sample chamber. (right) The diffraction image was taken at the ALS beamline 12.2.2 (non-ambient condition X-ray diffraction), and although the X-ray beam there (5x5 μm) is much larger than that at HPCAT (1x1 μm), it is more parallel in nature and we have taken the XRD pattern where the label H_2O is in the image above (left). There is minimal presence of rhenium as we move away from the flake.

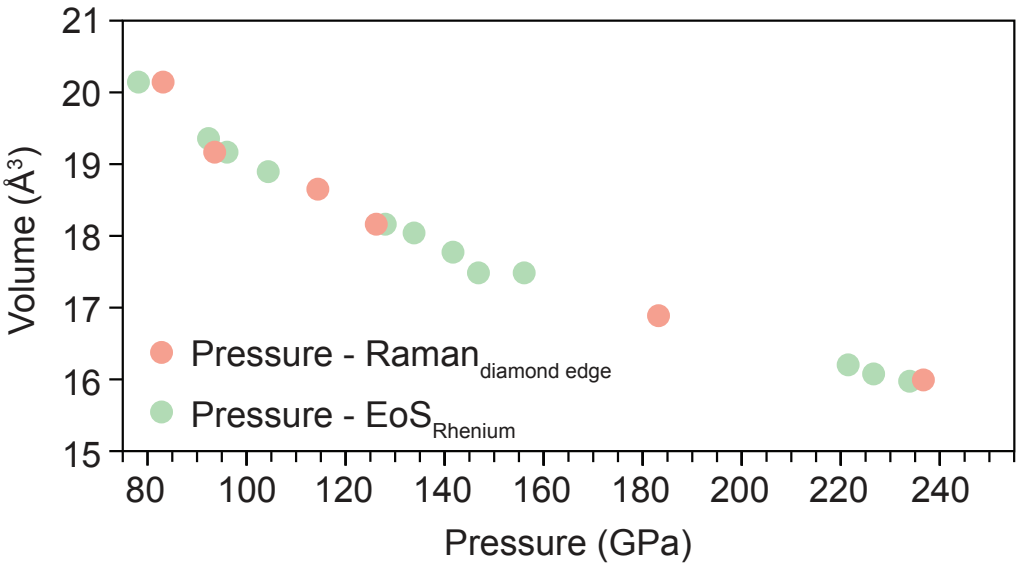

Figure 9. Volume-Pressure relations for water-ice. Pressure is determined using either (1) The strained diamond Raman edge (red), determined by the optical pressure scale of Akahama and Kawamura (2006) or (2) The Equation of state of rhenium (green) Anzellini et al. (2014)

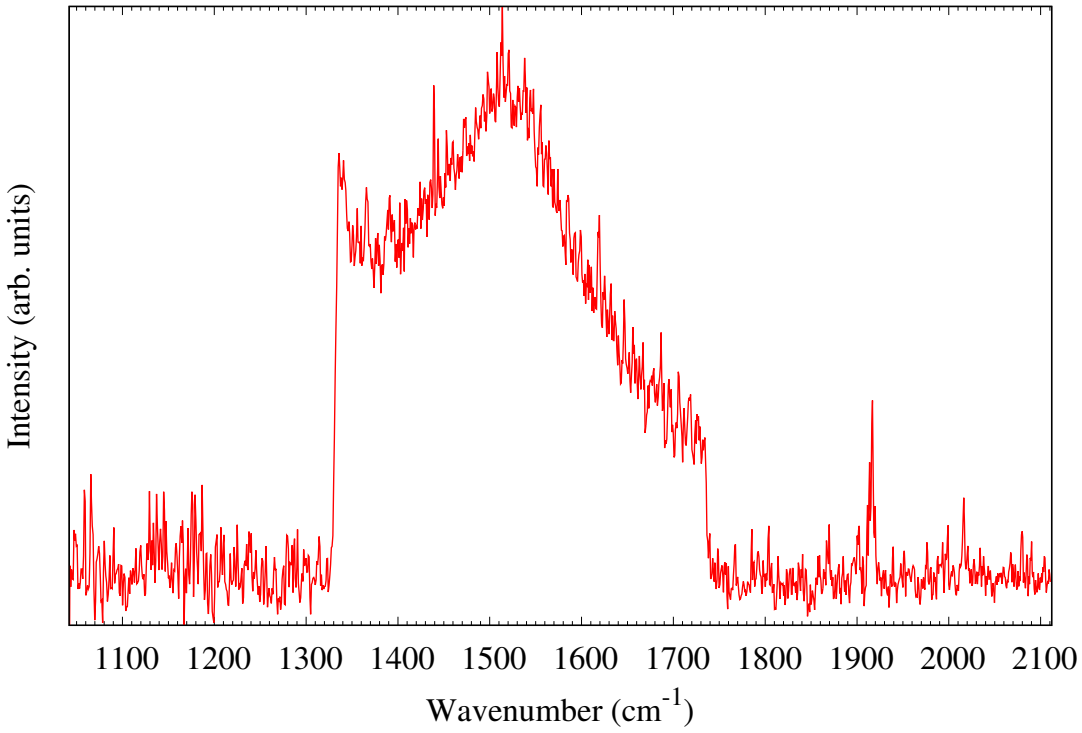

Figure 10. The diamond Raman edge was used to check pressure, whilst comparing to that determined by XRD using the equation of state of rhenium by Anzellini et al. (2014). This spectrum was collected at the highest pressure presented in this study, and is determined as 232 GPa by the optical pressure scale of Akahama and Kawamura (2006).

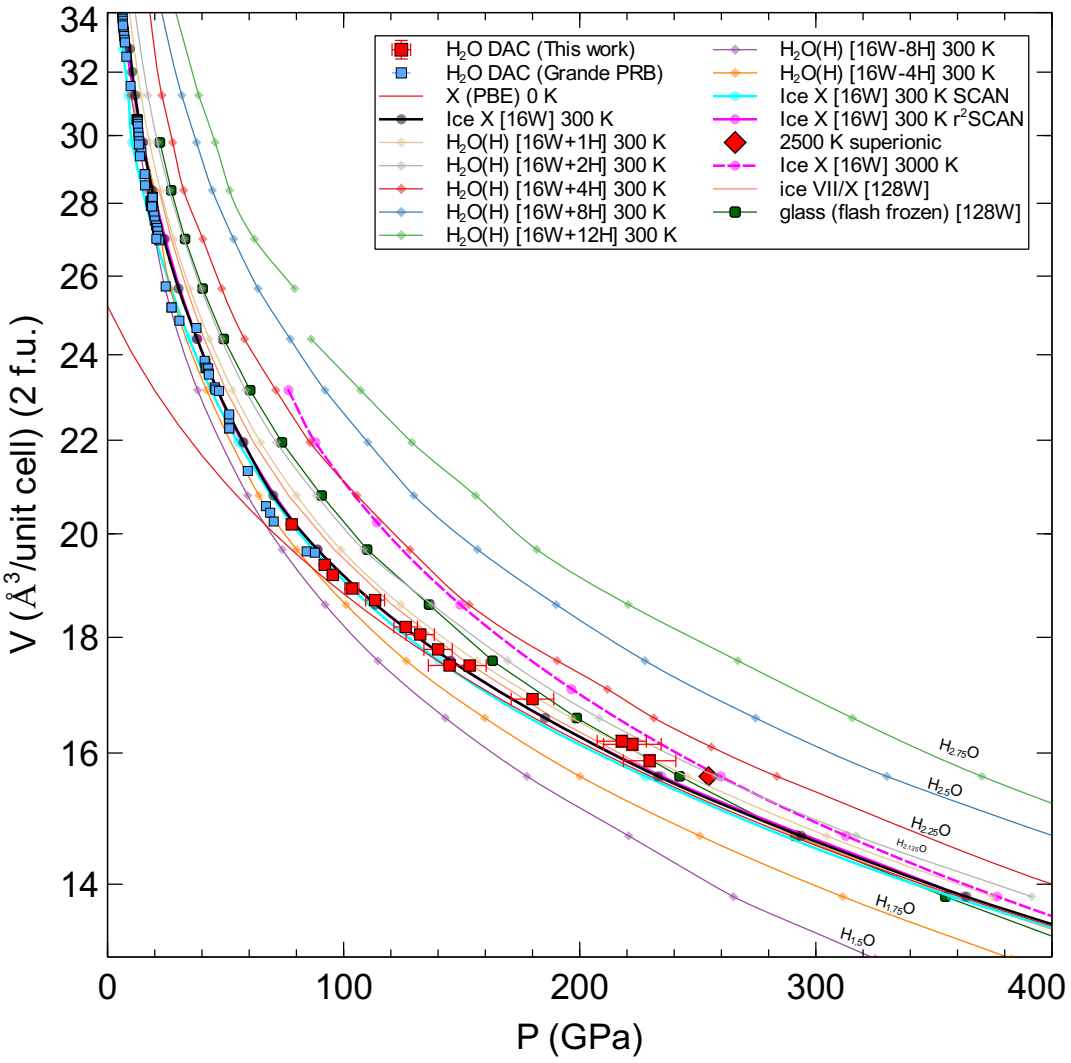

Figure 11. Calculated EOS of relevant ice phases, and temperatures, as a function of pressure. Underfilled and overfilled proton compositions of ice-VII/X were also simulated. Temperatures above 300 K provide an upperbound on the expected density, and simulations with more or less hydrogen (compared to the water 2:1 hydrogen:oxygen ratio) provide a guide in case the stoichiometry of the system changed at all with pressure. Similarly, glassy ice, which was formed by rapidly cooling liquid water and then simulating it at 300 K along this pressure range, provides an upperbound for ice as it should have a completely non-ideal structure (amorphous).

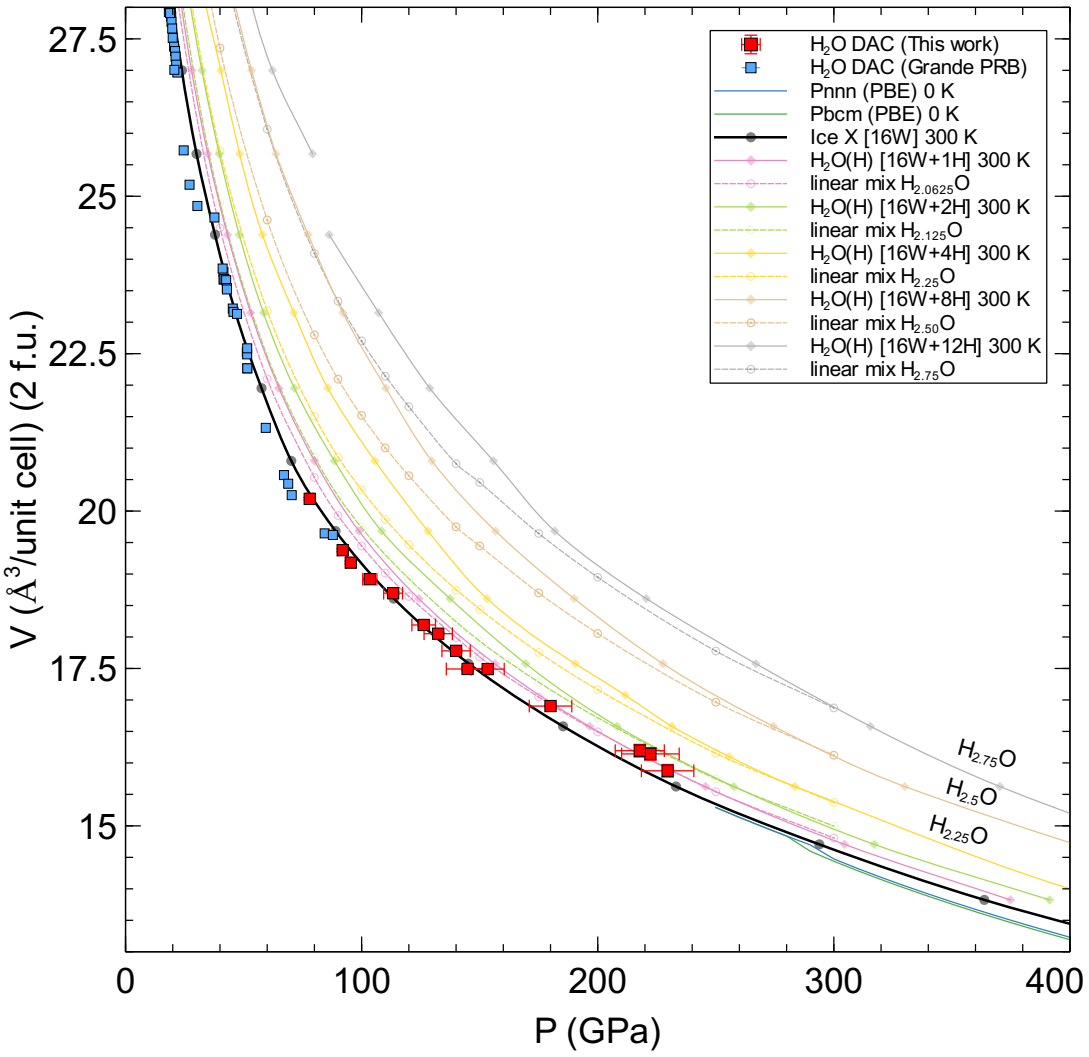

Figure 12. Calculated EOS of relevant ice phases, and temperatures, as a function of pressure. A linear mixing ratio volume (dashed lines) is also included here for comparison with the overfilled proton composition ice EOS data (by adding extra protons to ice-X). At lower pressures the linear mixture of H_2O and H tends to be less dense than the sum of its components, until around 300 GPa.

Table 1. Experientially determined pressure volume relations of H_2O-ice from this study. Pressure is determined from either the rhenium equation of state values by Anzellini et al. (2014), or the diamond Raman edge Akahama and Kawamura (2006).

P_{Eos-Re} (GPa)	$P_{Diamond-Raman}$	Phase	V_{H_2O} (Å^3)	a (Å)	b (Å)	c (Å)
230(11)	232(10)	$Pbcm$	15.91(3)	2.402(1)	3.700(2)	3.580(1)
		$P4_2/nnm$	15.99(1)	2.486(1)	2.588(2)	
222(12)		$Pbcm$	16.03(4)	2.409(1)	3.707(2)	3.590(2)
		$P4_2/nnm$	16.07(1)	2.501(1)	2.568(1)	
218(10)		$ice-X$	16.2(1)	2.5299(9)		
	180 (5)	$ice-X$	16.90(4)	2.566 (9)		
153(7)		$ice-X$	17.49(3)	2.5956(5)		
145(9)		$ice-X$	17.50(4)	2.5961(9)		
140(6)		$ice-X$	17.78(3)	2.6102(4)		
132(6)		$ice-X$	18.05(2)	2.623(1)		
126(5)	125(2)	$ice-X$	18.19(3)	2.6301(1)		
113(4)	113(2)	$ice-X$	18.70(2)	2.654(1)		
103(3)		$ice-X$	18.92(3)	2.665(1)		
95(2)		$ice-X$	19.18(2)	2.677(1)		
92(2)	93(2)	$ice-X$	19.38(2)	2.686(1)		
78(2)	83(2)	$ice-X$	20.19(2)	2.7232(9)		

Table 2. Experientially determined cell parameters of rhenium with compression. Pressure determined from volume relations from rhenium as described by the equation of state values by Anzellini et al. (2014), Dubrovinsky et al. (2012)

V_{Re} (Å^3)	a (Å)	c (Å)	c/a	$P_{Eos-Anzellini}$ (GPa)	$P_{Eos-Dubrovinsky}$ (GPa)
21.36(1)	2.4870(2)	3.990(2)	1.605	230(11)	284(16)
21.49(1)	2.4854(4)	4.018(3)	1.617	222(12)	274(17)
21.58(2)	2.4870(2)	4.028(1)	1.620	218(10)	267(15)
22.97(1)	2.5486(2)	4.086(4)	1.604	153(7)	180(10)
23.16(1)	2.5508	4.109(4)	1.611	145(9)	169(13)
23.30(1)	2.556(1)	4.116(4)	1.610	140(6)	163(8)
23.65(1)	2.569(1)	4.135(5)	1.609	132(6)	153(8)
23.41(2)	2.570(1)	4.099(2)	1.596	126(5)	145(7)
24.03(2)	2.586(1)	4.149(4)	1.605	113(4)	129(6)
24.33(1)	2.5953(8)	4.171(3)	1.607	103(3)	116(4)
24.60(1)	2.6026(9)	4.193(3)	1.611	95(2)	106(3)
24.71(1)	2.6077(9)	4.196(3)	1.609	92(2)	102(3)
25.21(1)	2.6246(8)	4.226(3)	1.610	78(2)	85(2)

REFERENCES

Akahama, Y. and Kawamura, H. (2006). Pressure calibration of diamond anvil raman gauge to 310 gpa. *Journal of Applied Physics*, 100(4):043516.

Anzellini, S., Dewaele, A., Occelli, F., Loubeyre, P., and Mezouar, M. (2014). Equation of state of rhenium and application for ultra high pressure calibration. *Journal of Applied Physics*, 115(4).

Dubrovinsky, L., Dubrovinskaia, N., Prakapenka, V. B., and Abakumov, A. M. (2012). Implementation of micro-ball nanodiamond anvils for high-pressure studies above 6 mbar. *Nature communications*, 3(1):1163.